Nitrogen Cycling

https://doi.org/10.48130/nc-0025-0013

Original Research

Open Access

Nitrification inhibitor enhances nitrogen use efficiency and crop yield more than biochar in calcareous soils

Lijun Liu[1,2,3], Nana Ding[1,2], Lei Meng[4], Qi Xu[1,2], Tongbin Zhu[1,2*], Ahmed S. Elrys[5,6], Lee Kheng Heng[7] and Christoph Müller[3,8]

Received: 31 October 2025

Revised: 29 November 2025

Accepted: 15 December 2025

Published online: 13 January 2026

Abstract

Calcareous soils are characterized by high pH and rapid nitrification, which often lead to excessive nitrate accumulation, nitrogen (N) loss, and increased nitrous oxide (N_2O) emissions. Effective inhibition of nitrification or enhancement of inorganic N retention is therefore crucial for enhancing N use efficiency (NUE) and mitigating N_2O emissions in such systems. Biochar and 3,4-dimethylpyrazole phosphate (DMPP) are widely used N management strategies; however, their relative effectiveness in improving NUE and mitigating N_2O emissions, as well as the underlying mechanisms regulating soil N transformations, remain poorly understood, particularly in calcareous soils. In this study, two consecutive seasons of pot experiments were conducted with eight treatments: control, phosphate and potash fertilizer (PK), N, phosphate and potash fertilizer (NPK), NPK + DMPP, NPK + low biochar (10 t ha^{-1}), NPK + high biochar (30 t ha^{-1}), NPK + low biochar + DMPP, and NPK + high biochar + DMPP. The effects of biochar and DMPP, applied alone, or in combination with, on crop N uptake, NUE, yield, soil gross N transformation rates, and N_2O emissions, were systematically evaluated. Results showed that DMPP significantly enhanced crop N uptake and yield by 30.8%–49.1% and 19.0%–48.9%, increased NUE by 14.4%–17.9%, and reduced cumulative N_2O emissions by 77.0%–85.1% relative to NPK across both seasons. Mechanistically, compared to NPK, DMPP effectively suppressed ammonia-oxidizing bacteria activity by 27.4%–42.4%, and nitrification rates by 50.0%–55.5%, but increased the microbial ammonium immobilization-to-nitrification ratio by 11.9%–20.8%, and prolonged the residence time of inorganic N, thereby enhancing N retention and utilization. In contrast, both low and high biochar additions promoted microbial N immobilization but accelerated nitrification, decreased NUE, and stimulated N_2O emissions; even co-application with DMPP did not counteract these effects. Overall, DMPP proved more effective than biochar in stabilizing inorganic N, improving NUE and crop yield, and mitigating N_2O emissions in calcareous soils, representing a key strategy for optimizing N management in such agroecosystems.

Keywords: Biochar, 3,4-dimethylpyrazole phosphate, Crop yield, N use efficiency, Gross N transformation rates, Soil N_2O emissions

Highlights

- DMPP was more effective than biochar in enhancing crop N uptake and yield in calcareous soils.
- DMPP outperformed biochar in improving N use efficiency and mitigating soil N_2O emissions.
- DMPP decreased nitrification and increased the ratio of microbial NH_4^+ immobilization to nitrification.
- DMPP exhibited a stronger effect than biochar in stimulating inorganic N retention in calcareous soil.

* Correspondence: Tongbin Zhu (zhutongbin@gmail.com)

Full list of author information is available at the end of the article.

https://doi.org/10.48130/nc-0025-0013

Graphical abstract

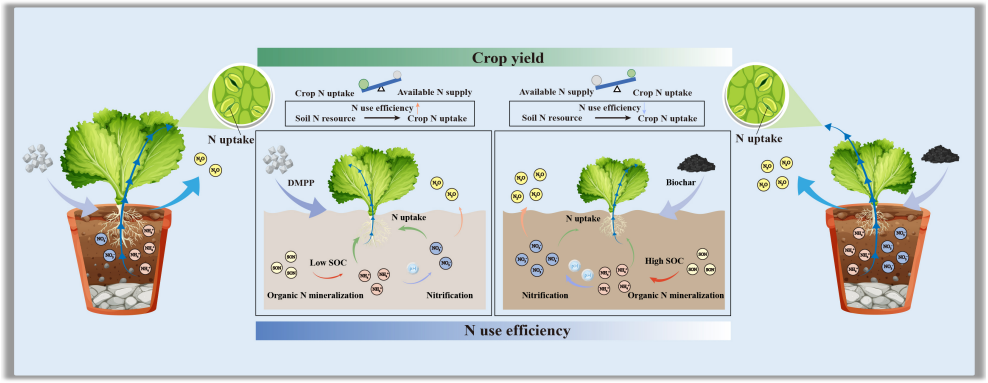

Introduction

Calcareous soils are among the most widely distributed agricultural soil types worldwide[1,2], predominantly distributed in the arid and semi-arid regions of Asia, the Mediterranean coast, North Africa, and southern Australia[3–5]. These soils are rich in carbonate minerals, which confer inherently high pH and calcium content, and play a vital role in maintaining regional food security, ecosystem stability, and agricultural sustainability[6–9]. However, their distinctive physicochemical properties also pose specific challenges for nitrogen (N) management[10,11]. A high pH environment favors the activity of ammonia-oxidizing bacteria (AOB) and accelerates nitrification, leading to rapid oxidation of ammonium (NH_4^+) to nitrate (NO_3^-)[12,13]. Consequently, inorganic N exhibits a short residence time within the soil system, while NO_3^- accumulates and is prone to leaching losses[10,14]. Under long-term intensive cultivation, farmers often rely on excessive N fertilizer inputs to compensate for N losses and sustain high crop yields[15,16]. Nevertheless, N use efficiency (NUE) in calcareous soils remains generally low[17,18]. Excessive N input not only escapes crop uptake but also leads to NO_3^- loss through leaching and denitrification, resulting in the emission of gaseous N forms such as nitrogen gas (N_2) and nitrous oxide (N_2O)[19]. These processes collectively contribute to severe agricultural non–point source pollution and greenhouse gas emissions[11,16,20]. Such a 'high input–low utilization–high loss' N cycle pattern diminishes fertilizer benefits, and threatens both the regional ecological security and climate regulation.

To address the pervasive issues of high N losses and low use efficiency in calcareous soils, reducing nitrification rates and delaying the conversion of NH_4^+ to NO_3^-, represent effective strategies for mitigating N loss[11,12]. Meanwhile, enhancing the retention and recycling of inorganic N within the soils is a core approach to improving NUE[10,21]. The former strategy focuses on suppressing ammonia oxidation and the related processes to limit nitrification rates, thereby reducing NO_3^- accumulation and its subsequent leaching losses[22]. The latter relies on promoting microbial immobilization and adsorption processes, extending N residence time within the soil–plant system to achieve more efficient N retention and recycling[23,24]. A thorough comprehension of these processes is crucial for optimizing soil N cycling and enhancing agricultural NUE. Among current N management strategies, biochar and nitrification inhibitors are among the most promising approaches for simultaneously reducing N losses and improving NUE through distinct mechanisms[25–27]. Biochar, a carbon (C) rich porous material that can improve soil physicochemical properties, such as organic C content, cation exchange capacity, and water-holding capacity (WHC), thereby enhancing crop N uptake[28–30]. Meanwhile, its abundant surface functional groups (e.g., carboxyl, hydroxyl, and phenolic hydroxyl groups) significantly enhance the adsorption and retention of NH_4^+, delaying its oxidation by nitrifying microbes and thus stabilizing the soil inorganic N pool[24,31]. Furthermore, certain biochars contain volatile or aromatic organic compounds that may exert mild inhibitory effects on AOB, indirectly suppressing nitrification[31,32]. In contrast, the nitrification inhibitor 3,4-dimethylpyrazole phosphate (DMPP) directly inhibits the activity of both AOB and ammonia-oxidizing archaea (AOA) by chelating copper ions at the active site of ammonia monooxygenase (AMO), thus delaying NH_4^+ oxidation and substantially reducing NO_3^- formation and N_2O emissions[33,34]. Importantly, DMPP exhibits high chemical stability under high pH conditions and is particularly effective in calcareous soils, where nitrification is predominantly driven by AOB[11,35,36].

Although both biochar and DMPP have demonstrated positive effects in reducing N losses, their effectiveness is strongly influenced by application rate, method, and soil environmental conditions[37–39]. Studies have indicated that low biochar application rates generally enhance microbial activity, promote organic N mineralization and microbial immobilization, and thereby facilitate N retention and transformation[40,41]. In contrast, high biochar application rates may alter soil oxygen diffusion and microbial community composition, accelerating nitrification and consequently increasing N losses[41,42]. The co-application of biochar and DMPP is considered to provide dual benefits: physical retention and biochemical inhibition[38,39]. However, research on their interactive mechanisms remains limited, with most studies focusing primarily on crop yield and soil N_2O emissions[37,38,43]. In contrast, systematic quantification of key processes such as NH_4^+ immobilization, nitrification rates, and NO_3^- accumulation remains lacking. Overall, current studies on the combined use of biochar and nitrification inhibitors in calcareous soils reveals substantial knowledge gaps concerning application rate-dependent effects, synergistic mechanisms, and the quantitative dynamics of N transformation processes. Elucidating the dynamic characteristics, rate-limiting steps, and underlying biogeochemical drivers of N transformations in calcareous soils will not only advance theoretical frameworks for efficient N retention and utilization but also provide an essential scientific foundation for establishing precision N management strategies and achieving sustainable agricultural production.

Therefore, this study used a typical calcareous soil as the research object, and pak choi (*Brassica rapa*) as the test crop. Eight experimental treatments were conducted to assess the individual and combined effects of biochar and DMPP at different application

rates: control (CK), phosphate and potash fertilizer (PK), N, phosphate, and potash fertilizer (NPK), NPK + DMPP, NPK + low biochar (10 kg ha^{-1}), NPK + high biochar (30 kg ha^{-1}), NPK + low biochar + DMPP, and NPK + high biochar + DMPP. A two-season pot experiment was conducted to systematically assess how these amendments influence crop yield, N uptake, and NUE, soil inorganic N turnover processes, the abundance of N-cycling functional genes, and N_2O emissions. The present study aimed to address the following questions: (1) How do individual and combined applications of biochar and DMPP affect crop yield, N uptake, and NUE in calcareous soil? (2) How do these treatments regulate soil N availability, gross N transformation processes, and N losses, particularly N_2O emissions? The present results will offer a theoretical foundation for optimizing N fertilizer management, enhancing NUE, and mitigating agricultural greenhouse gas emissions in calcareous soils, thereby promoting sustainable crop production.

Materials and methods

Study site and material preparation

The experimental soil was sampled from Nanxu Village, Lingchuan County, Guilin City, Guangxi Zhuang Autonomous Region, China (25°08'51" N, 110°50'36" E). The region has a typical subtropical monsoon climate, with a mean annual temperature of 18.7 °C, and a mean annual precipitation of 1,942 mm, mainly occurring between April and July. It receives approximately 1,615 h of annual sunshine, and has a frost-free period of about 349 d. The sampling site had been under continuous citrus cultivation for five years, with average annual fertilizer inputs of 256 kg N ha^{-1}, 96.0 kg P_2O_5 ha^{-1}, and 209 kg K_2O ha^{-1}. Soil samples were obtained in September 2023 from depths of 0–20 cm and 20–40 cm. Visible plant residues and gravel were removed, after which the samples were air-dried and passed through a 5 mm sieve before analysis. The experimental soil belongs to calcareous soil and had the following basic physicochemical properties: pH 8.20, soil organic C 19.2 g C kg^{-1}, total N 2.00 g N kg^{-1}, available phosphorus (P) 1.38 g kg^{-1}, available potassium (K) 7.71 g kg^{-1}, and total calcium 134.6 g kg^{-1}.

The biochar for this experiment was provided by the School of Environmental and Ecological Engineering, Jiangnan University. It was produced from camphor wood (*Cinnamomum camphora*) through pyrolysis under anaerobic conditions at 500–550 °C. The biochar had a pH of 7.10, total C 261 g C kg^{-1}, and total N 2.70 g N kg^{-1}. The nitrification inhibitor DMPP (98% purity) was supplied by Zhengzhou Shenyu Chemical Co., Ltd. The test crop was pak choi (*Brassica rapa*), cultivar 'Guixing', provided by Guangzhou Mingxin Agricultural Technology Co., Ltd.

Pot experiment design

The pot experiment was conducted in October 2023, in a greenhouse at the International Karst Research Center in Guilin City. Rigid polyvinyl chloride (PVC) pots (30 cm diameter × 60 cm height) served as cultivation containers. Before filling, all pots were thoroughly rinsed with clean water and air-dried to avoid any contamination. The soils were filled into the pots according to the original stratification of the sampled layers. A 10 cm layer of calcareous gravel was placed at the bottom of each pot to facilitate drainage and aeration, followed by air-dried and sieved soil. Each pot was filled with approximately 14.5 kg of soil. To maintain a bulk density consistent with field conditions, the soil was gently compacted every 5 cm during filling to ensure uniformity. This study set up biochar and nitrification inhibitor treatments to evaluate their effects on decreasing N loss and enhancing NUE. The biochar application was primarily aimed at testing whether it could stimulate the retention of inorganic N and reduce N loss, while the nitrification inhibitor was applied to verify its ability to decrease nitrification rates, increase NH_4^+ retention, and improve NUE. Eight treatments were established (Supplementary Table S1): (1) CK, no fertilizer (control); (2) PK, P, and K fertilizers only; (3) NPK, N, P, and K fertilizers; (4) NPK + DMPP, NPK fertilizers plus DMPP; (5) NPK + BC10, NPK fertilizers plus 10 t ha^{-1} biochar; (6) NPK + BC30, NPK fertilizers plus 30 t ha^{-1} biochar; (7) NPK + BC10 + DMPP, NPK fertilizers plus 10 t ha^{-1} biochar and DMPP; and (8) NPK + BC30 + DMPP, NPK fertilizers plus 30 t ha^{-1} biochar and DMPP. Each treatment had three replicates, resulting in 24 pots arranged in a randomized complete block design. Fertilization was based on local conventional practices, with application rates equivalent to 256 kg N ha^{-1} (urea), 96.0 kg P_2O_5 ha^{-1} (superphosphate), and 209 kg K_2O ha^{-1} (potassium sulfate). The DMPP application rate was equivalent to 1.50% of the pure N content from urea. Biochar was added at rates of 10 and 30 t ha^{-1}. All fertilizers, DMPP, and biochar were thoroughly mixed with the soil prior to sowing and applied once as a basal dressing. After fertilization, the pots were irrigated to approximately 60% WHC and equilibrated for 48 h before sowing. Twenty seeds of pak choi were sown per pot, and after emergence, seedlings were thinned to retain three uniform plants per pot based on growth vigor. During the growth period, soil moisture was maintained uniformly across all pots through manual watering, and no additional fertilizer was applied. The first growing season lasted from October 23, 2023, to January 20, 2024, and the second from February 20, 2024, to May 1, 2024. Identical cultivation and management practices were used for both seasons.

Plant sample collection and nutrient analysis

At maturity, pak choi plants were harvested. The aboveground and belowground parts were washed separately with deionized water, and their fresh weights were measured. The plant samples were then placed in cloth bags, inactivated at 105 °C for 30 min, and subsequently oven-dried at 80 °C to a constant weight to determine the dry biomass of both aboveground and belowground components. The dried samples were ground into fine powder using an AM410 planetary ball mill (Beijing Grinder Instrument Co., Ltd, China). Total C and N contents of the aboveground and belowground samples were analyzed with a Sercon Integra 2 isotope ratio mass spectrometer (Sercon Ltd., Crewe, UK).

Crop NUE (%) was determined as follows:

$$N_{uptake} = \text{Total dry weight} \times \text{Total N content} \quad (1)$$

$$NUE = \frac{N_{uptake1} - N_{uptake0}}{C_{Nf}} \times 100 \quad (2)$$

where, N_{uptake} is the total crop N uptake, mg; $N_{uptake1}$ and $N_{uptake0}$ are the total crop N uptake in fertilized and unfertilized treatments, mg; and C_{Nf} is the amount of N fertilizer added to each treatment, mg pot^{-1}.

Soil N_2O emission collection and determination

Soil N_2O emissions were determined using the static closed chamber–gas chromatography method beginning on October 31, 2023. The sampling system comprised a sealed opaque chamber (40 cm height × 30 cm diameter), and a PVC base frame. The chamber was equipped with a gas sampling port and a temperature sensor at the top. The base frame featured a square structure with a 5 cm-wide annular water channel along its edges to create a water seal during sampling. Before sampling, the chamber was securely installed above the pot, and the base channel was filled with deionized water to ensure the system was airtight. A small fan inside the chamber was operated during sampling to ensure uniform gas mixing. To minimize the effects of light and

https://doi.org/10.48130/nc-0025-0013

temperature fluctuations on gas exchange, all sampling was consistently conducted between 08:00 and 11:00. To ensure homogeneity, the chamber air was pre-flushed 3–5 times prior to sampling. Gas samples were collected from the chamber headspace using a 25 mL gas syringe at 0, 10, 20, and 30 min after chamber closure and immediately transferred into 20 mL pre-evacuated glass vials. Chamber and ambient air temperatures were recorded simultaneously. Sampling was performed on days 1, 2, 3, 5, and 7 after fertilization, and subsequently once per week until pak choi harvest. N_2O concentrations were determined using an Agilent 7890A gas chromatograph (Agilent Technologies, USA) fitted with an electron capture detector (ECD). High-purity N_2 (> 99.9%) served as the carrier gas. The column, detector, and injector temperatures were set to 55, 350, and 100 °C, respectively.

The N_2O emission flux (F, mg kg^{-1} h^{-1}), cumulative N_2O emission (M, mg kg^{-1}), yield-scaled N_2O emission (mg kg^{-1} yield), and N_2O emission factor (EF, %) were calculated as follows:

$$F = \rho \times \frac{\Delta C}{\Delta t} \times \frac{273.15}{(273.15 + T)} \times \frac{V}{A} \quad (3)$$

$$M = F_1 \times 24 + \sum_{i=2}^{n} \frac{F_i + F_{i-1}}{2} (t_i - t_{i-1}) \times 24 \quad (4)$$

$$\text{Yield-scaled } N_2O \text{ emission} = \frac{M}{\text{Yield}} \quad (5)$$

$$EF = \frac{M_n - M_c}{F_N} \times 100\% \quad (6)$$

where, ρ is the N_2O density under standard conditions, kg m^{-3}; $\Delta C/\Delta t$ is the rate of change in N_2O concentration during the sampling period; T is the chamber temperature, °C; V is the adequate chamber volume, m^3; A is the chamber base area, m^2; $t_i - t_{i-1}$ are consecutive sampling times, d; n is the total number of samplings; Yield is the dry weight of pak choi per season; M_n and M_c are the cumulative N_2O emissions from fertilized and unfertilized soil, kg ha^{-1}; and F_N is the amount of N fertilizer added to each treatment, kg N ha^{-1}.

Soil sample collection and physicochemical properties determination

After pak choi harvest, soil samples were immediately obtained from each pot. Five soil cores (5 cm in diameter) were sampled from the 0–10 cm surface layer of each pot using a five-point sampling method. After removing visible plant residues, roots, and other debris, the soil cores from each pot were thoroughly homogenized to obtain a composite sample. The composite soil was sieved through a 2 mm mesh and divided into three subsamples: one portion was refrigerated at 4 °C for determining gross N transformation rates; the second portion was frozen at –80 °C for quantifying N-cycling functional gene abundances; and the remaining portion was air-dried for basic physicochemical properties determination.

Soil pH was analyzed in a 1:2.5 (w/v) soil-water suspension with a SevenExcellence pH/mV meter. Soil WHC was measured by saturating soil samples with deionized water for 2 h, followed by natural filtration for 7 h[44]. Soil organic C and total N contents were measured using a Sercon Integra 2 isotope ratio mass spectrometer (Sercon Ltd., Crewe, UK) after pretreatment with 1 mol L^{-1} hydrohloric acid (HCl)[13]. Soil NH_4^+ and NO_3^- contents were determined with a flow analyzer (Skalar, Breda, The Netherlands). For determining the isotopic abundances of NH_4^+ and NO_3^-, the extraction solutions were pretreated using the magnesium oxide (MgO)-Devarda alloy distillation method[45]. In brief, MgO was first added to the extract to distill NH_4^+, followed by the addition of Devarda's alloy to reduce NO_3^- to NH_4^+ for subsequent distillation. The distillates were collected in a boric acid solution containing mixed indicators (methyl red and bromocresol green) and titrated with 0.02 mol L^{-1} sulfuric acid. The resulting solution was oven-dried at 80 °C and analyzed for ^{15}N isotopic abundance using the Sercon Integra 2 mass spectrometer.

Soil ^{15}N tracing experiment

A series of fresh soil samples (30 g dry weight equivalent) was placed into 250 mL Erlenmeyer flasks and pre-incubated at 25 °C for 24 h. After pre-incubation, the soils were divided into two groups. Each flask received 1 mL of either $^{15}NH_4NO_3$ (5.22 atm% ^{15}N excess) or $NH_4{}^{15}NO_3$ (5.14 atm% ^{15}N excess) solution, uniformly applied to the soil surface, providing 50 mg N kg^{-1} NH_4^+ and 50 mg N kg^{-1} NO_3^-, respectively. Soil moisture was adjusted to 60% WHC, and the flasks were sealed with perforated parafilm to allow gas exchange. The samples were then incubated continuously at 25 °C. At 0.5 and 24 h after the addition of the ^{15}N tracer, inorganic N was extracted with 150 mL of 2 mol L^{-1} potassium chloride (KCl) solution. The contents of NH_4^+ and NO_3^-, as well as their respective ^{15}N enrichments, were determined in the extracts.

Gross rates of N transformation, including gross N mineralization (GNM), gross nitrification (GN), gross NH_4^+ immobilization (GAI), and gross NO_3^- immobilization (GNI) (mg N kg^{-1} d^{-1}), were evaluated as follows[46]:

$$m = \frac{M_0 - M_1}{t_1 - t_0} \times \frac{\ln\left(\frac{H_0 M_1}{H_1 M_0}\right)}{\ln\left(\frac{M_0}{M_1}\right)}, \; c \neq m \quad (7)$$

$$c = \frac{M_0 - M_1}{t_1 - t_0} \times \frac{\ln\left(\frac{H_0}{H_1}\right)}{\ln\left(\frac{M_0}{M_1}\right)}, \; c \neq m \quad (8)$$

where, M_0 and M_1 are the contents of N at times t_0 and t_1 (NH_4^+ for $^{15}NH_4^+$-labeled soils and NO_3^- for $^{15}NO_3^-$-labeled soils), and H_0 and H_1 are the corresponding ^{15}N atom values. Here, m represents the GNM for $^{15}NH_4^+$-labeled soil or the GN for $^{15}NO_3^-$-labeled soil, while c represents the NH_4^+ consumption rate in $^{15}NH_4^+$-labeled soil or the GNI in $^{15}NO_3^-$-labeled soil. The GAI was calculated as the difference between the NH_4^+ consumption rate and GN, and gross microbial immobilization rate was obtained by summing GAI and GNI.

The mean residence time (MRT) represents the turnover rate of the inorganic N pool, with greater values suggesting slower turnover[47]. MRTs of NH_4^+ (MRT NH_4^+) and NO_3^- (MRT NO_3^-) were determined as follows:

$$\text{MRT } NH_4^+ = \frac{C(NH_4^+)}{GNM} \quad (9)$$

$$\text{MRT } NO_3^- = \frac{C(NO_3^-)}{GN} \quad (10)$$

where, $C(NH_4^+)$ and $C(NO_3^-)$ are the initial soil contents of NH_4^+ and NO_3^-, mg N kg^{-1}.

Soil DNA extraction, quantitative PCR, and high-throughput sequencing

Total DNA was obtained from each soil sample using the FastDNA® Spin Kit for Soil (MP Biomedicals, Cleveland, OH, USA) according to the manufacturer's instructions. DNA purity and concentration were analyzed with a NanoDrop 2000c spectrophotometer (Thermo Fisher Scientific, USA), after which the extracts were stored at –20 °C for further analysis. The abundances of AOB and AOA *amoA* genes

were quantified by quantitative real-time PCR (qPCR). The primer pairs used were *amoA*-F (5'-GGGGTTTCTACTGGTGGT-3')/*amoA*-R (5'-CCCCTCKGSAAAGCCTTCTTC-3') for AOB, and Arch-*amoA*-F (5'-STAA TGGTCTGGCTTAGACG-3')/Arch-*amoA*-R (5'-GCGGCCATCCATCTGTAT GT-3') for AOA. Each 30 μL qPCR reaction included 15 μL SYBR Green qPCR Master Mix (Takara, Japan), 2 μL Mg^{2+} solution, 0.5 μL of each primer (10 μmol L^{-1}), 2 μL of template DNA, 0.5 μL fluorescent dye, and ddH_2O to a final volume. Thermal cycling conditions were as follows: For AOB *amoA*, 95 °C for 3 min (initial denaturation), followed by 40 cycles of 94 °C for 15 s, 60 °C for 30 s, and 72 °C for 30 s. For AOA *amoA*, 95 °C for 3 min (initial denaturation), followed by 40 cycles of 94 °C for 15 s, 60 °C for 20 s, and 72 °C for 20 s. All reactions were performed in triplicate, and melting curve analysis confirmed amplification specificity. The amplification efficiency ranged from 90% to 110%, with $R^2 > 0.99$ for all standard curves. PCR amplification was carried out on an ABI GeneAmp® 9700 thermal cycler (Applied Biosystems, USA). Amplicon specificity and expected fragment size were verified by 2% agarose gel electrophoresis, and the target bands were purified with a DNA Gel Extraction Kit (Omega Bio-Tek, USA). Purified amplicons were determined with a Qubit 4.0 fluorometer (Thermo Fisher Scientific, USA) and pooled in equimolar amounts. Sequencing libraries were constructed via end repair, A-tailing, adapter ligation, and PCR enrichment. High-throughput sequencing was then performed on an Illumina HiSeq 2500 platform (Illumina, USA).

Data analysis

Before statistical analyses, the Shapiro–Wilk test was carried out to examine data normality. When normality assumptions were not met, data were transformed using a standard score transformation method to eliminate heteroscedasticity. Following transformation, one-way analysis of variance (ANOVA), followed by the least significant difference (LSD) test ($p < 0.05$) was performed to compare differences in plant traits, soil physicochemical and microbial properties, inorganic N turnover rates, and N_2O emissions among fertilization treatments within each growing season. Differences in these variables between the two growing seasons were analyzed using independent-samples *t*-tests ($p < 0.05$). A two-way ANOVA was applied to evaluate the impacts of fertilization, growing season, and their interaction on all measured parameters (Supplementary Table S2). A Pearson correlation analysis was performed to examine relationships among plant traits, soil physicochemical and microbial properties, inorganic N turnover rates, and N_2O emissions. All statistical analyses were carried out using Origin 2021 Pro (OriginLab Corporation, Northampton, MA, USA) and Adobe Illustrator. Data are expressed as means ± standard deviation ($n = 3$).

Results

Crop yield, nutrient content, N uptake, and NUE

Crop yield, nutrient content, N uptake, and NUE were greatly altered by fertilization treatments, growing seasons, and their interactions (Fig. 1; Supplementary Fig. S1). The NPK + DMPP and NPK + BC10 treatments significantly increased total crop yield in both seasons, with NPK + DMPP showing a more pronounced effect. Across both seasons, NPK + DMPP consistently produced higher total crop yield than NPK + BC10 and NPK + BC10 + DMPP. Total crop yield under NPK + BC10 was significantly higher than under NPK + BC30 in the second season. Crop N content under NPK + DMPP was significantly higher than under NPK + BC10, NPK + BC30, and NPK + BC30 + DMPP in the first season. Meanwhile, NPK + BC10 resulted in significantly lower crop N content than NPK + BC30 in the first season. Across both seasons, NPK + DMPP significantly enhanced crop N uptake, which remained significantly higher than that under NPK + BC10. Crop N uptake under NPK + BC10 was significantly lower than under NPK + BC30 in the first season. Across both seasons, NUE was highest under NPK + DMPP and lowest under NPK + BC30. NUE under NPK + DMPP consistently exceeded that under NPK + BC30 in both seasons, and NUE under NPK + BC10 also remained higher than under NPK + BC30.

Soil physicochemical properties

Fertilization treatments, growing seasons, and their interactions significantly affected soil physicochemical properties (Table 1). NPK + DMPP, NPK + BC10, NPK + BC10 + DMPP, and NPK + BC30 + DMPP

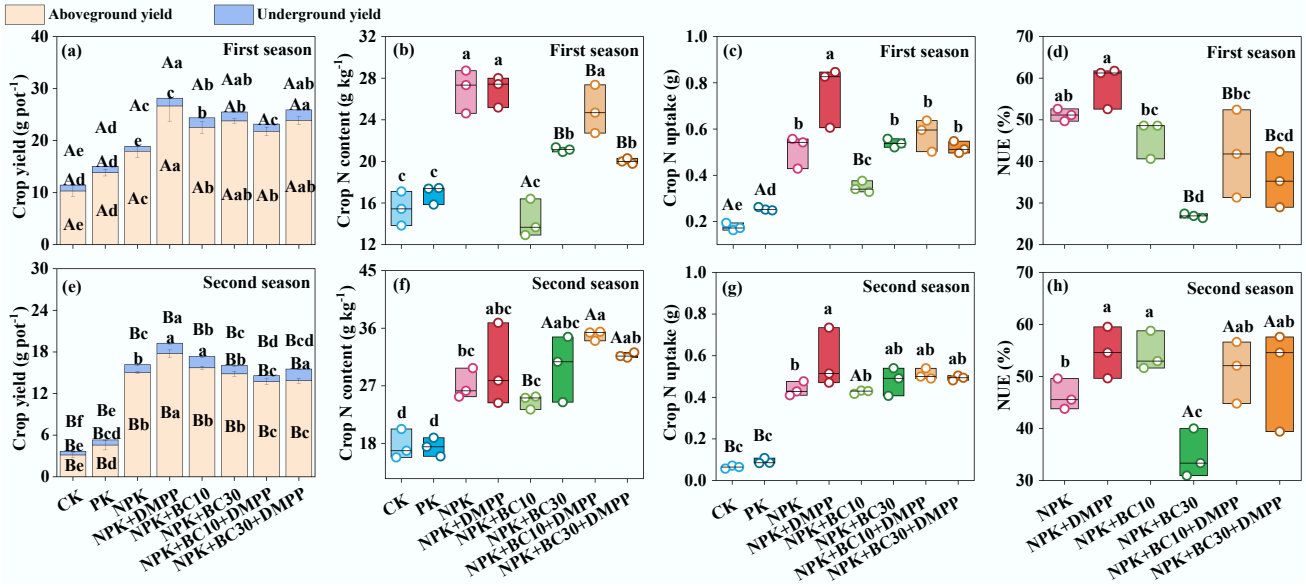

Fig. 1 Changes in (**a**), (**e**) crop yield, (**b**), (**f**) crop N content, (**c**), (**g**) crop N uptake, (**d**), (**h**) NUE after fertilizer application during the first and second seasons. Different lowercase and uppercase letters indicate significant differences between fertilization treatments and growing seasons, respectively. The absence of letters indicates no significant differences. The values represent the average ± standard deviation ($n = 3$).

https://doi.org/10.48130/nc-0025-0013

significantly decreased soil pH across both seasons. In contrast, NPK + BC30 and NPK + BC30 + DMPP significantly enhanced soil organic C content and the C/N ratio in both seasons, and also significantly elevated soil NO_3^- and inorganic N contents during the second season. Soils under NPK + DMPP exhibited significantly lower pH, soil organic C content, and C/N ratio than those under NPK + BC10, NPK + BC30, NPK + BC10 + DMPP, and NPK + BC30 + DMPP in both seasons, with the differences more pronounced under NPK + BC30. Furthermore, soil pH was consistently lower under NPK + BC10 than under NPK + BC30 across both seasons.

Soil N_2O emissions, yield-scaled N_2O emissions, and N_2O emission factors

Fertilization treatments, growing seasons, and their interactions significantly affected soil N_2O emissions, yield-scaled N_2O emissions, and N_2O emission factors (Fig. 2; Supplementary Fig. S2). Overall, NPK + DMPP, NPK + BC10, and NPK + BC10 + DMPP significantly decreased soil N_2O emissions across both seasons, with the strongest mitigation observed under NPK + DMPP. In contrast, NPK + BC30 and NPK + BC30 + DMPP significantly reduced N_2O emissions only in the second season. N_2O emissions under NPK + BC10 were significantly reduced relative to NPK + BC30 in the first season, whereas the opposite trend was

Table 1 Changes in soil physicochemical properties after fertilizer application during the first and second seasons

Paramenter[a]	Season	CK	PK	NPK	NPK + DMPP	NPK + BC10	NPK + BC30	NPK + BC10 + DMPP	NPK + BC30 + DMPP
WHC (%)	First	63.9 ± 0.21a	57.2 ± 5.84b	62.6 ± 4.27Ba	60.3 ± 3.02Bab	60.7 ± 3.97ab	61.7 ± 1.01ab	63.0 ± 1.87a	58.3 ± 1.70ab
	Second	64.4 ± 0.30	65.1 ± 1.65	65.7 ± 0.27A	64.1 ± 0.12A	65.5 ± 2.58	59.1 ± 7.02	58.7 ± 9.13	55.9 ± 9.76
pH	First	8.25 ± 0.14b	8.35 ± 0.05Ab	8.44 ± 0.03Aa	7.95 ± 0.04d	8.04 ± 0.02Ac	8.33 ± 0.09Ab	8.05 ± 0.01Ac	8.25 ± 0.09b
	Second	8.13 ± 0.03ab	8.15 ± 0.03Bab	8.17 ± 0.04Ba	7.90 ± 0.05d	7.99 ± 0.02Bcd	8.14 ± 0.04Bab	8.01 ± 0.01Bc	8.09 ± 0.02bc
Soil organic C ($g\ C\ kg^{-1}$)	First	51.9 ± 2.37d	51.1 ± 0.77d	53.5 ± 0.40c	50.2 ± 3.26d	57.5 ± 0.36b	67.9 ± 0.22Aa	58.7 ± 1.65b	68.2 ± 0.75a
	Second	52.4 ± 1.22c	50.0 ± 2.58d	51.8 ± 1.89cd	49.3 ± 2.51d	57.9 ± 0.59b	63.8 ± 1.19Ba	56.6 ± 1.60bc	65.2 ± 3.37a
Total N ($g\ N\ kg^{-1}$)	First	2.13 ± 0.02B	2.12 ± 0.04	2.06 ± 0.04	2.10 ± 0.08	2.19 ± 0.08	2.17 ± 0.11	2.10 ± 0.03	2.09 ± 0.01
	Second	2.17 ± 0.00Aab	2.16 ± 0.04ab	2.17 ± 0.08ab	2.10 ± 0.03b	2.20 ± 0.02ab	2.25 ± 0.02a	2.13 ± 0.05ab	2.18 ± 0.12ab
C/N	First	24.4 ± 1.18c	24.1 ± 0.58c	26.0 ± 0.50bc	23.9 ± 2.33c	26.3 ± 1.13bc	31.4 ± 1.56Aa	28.0 ± 1.16b	32.7 ± 0.30Aa
	Second	24.2 ± 0.59cd	23.1 ± 1.35d	23.9 ± 1.19d	23.4 ± 0.88d	26.3 ± 0.46bc	28.3 ± 0.25Bab	26.6 ± 1.30b	29.9 ± 0.06Ba
NH_4^+ ($mg\ N\ kg^{-1}$)	First	3.87 ± 1.09c	5.07 ± 0.45abc	4.92 ± 0.59abc	5.39 ± 0.22abc	6.82 ± 0.98a	5.87 ± 0.59ab	5.87 ± 1.57abc	4.28 ± 0.67bc
	Second	4.92 ± 0.37b	4.92 ± 0.14b	4.73 ± 0.48b	6.50 ± 0.64a	5.71 ± 1.00ab	4.82 ± 0.28b	6.01 ± 0.74ab	5.61 ± 0.42ab
NO_3^- ($mg\ N\ kg^{-1}$)	First	6.66 ± 1.03B	7.45 ± 1.47B	8.56 ± 2.02B	6.50 ± 0.98B	7.61 ± 2.06B	7.93 ± 0.81B	7.93 ± 0.22B	5.71 ± 1.03B
	Second	12.4 ± 0.24Ade	11.0 ± 0.85Ae	15.2 ± 1.24Acd	15.0 ± 2.80Acd	15.9 ± 0.97Abcd	20.5 ± 2.91Aa	19.5 ± 2.96Aabc	20.3 ± 1.24Aab
Inorganic N ($mg\ N\ kg^{-1}$)	First	10.5 ± 2.09Bab	12.5 ± 1.25Bab	13.5 ± 1.47Bab	11.9 ± 0.78Bab	14.4 ± 3.02Ba	13.8 ± 1.40Ba	13.8 ± 1.35Ba	9.99 ± 1.69Bb
	Second	17.3 ± 0.14Acd	16.0 ± 0.96Ad	19.9 ± 1.45Abc	21.5 ± 2.19Ab	21.6 ± 0.87Aab	25.3 ± 2.66Aa	25.5 ± 2.34Aa	25.9 ± 1.39Aa
NO_3^-/NH_4^+	First	1.80 ± 0.30B	1.49 ± 0.38	1.81 ± 0.58B	1.21 ± 0.22	1.10 ± 0.14B	1.35 ± 0.01B	1.45 ± 0.36B	1.33 ± 0.05B
	Second	2.54 ± 0.25Abc	2.24 ± 0.12c	3.23 ± 0.33Aabc	2.37 ± 0.71c	2.87 ± 0.56Abc	4.29 ± 0.86Aa	3.36 ± 0.95Aabc	3.63 ± 0.31Aab

[a] WHC, water holding capacity. Different lowercase and uppercase letters indicate significant differences between fertilization treatments and growing seasons, respectively. The absence of letters indicates no significant differences. The values represent the average ± standard deviation ($n = 3$).

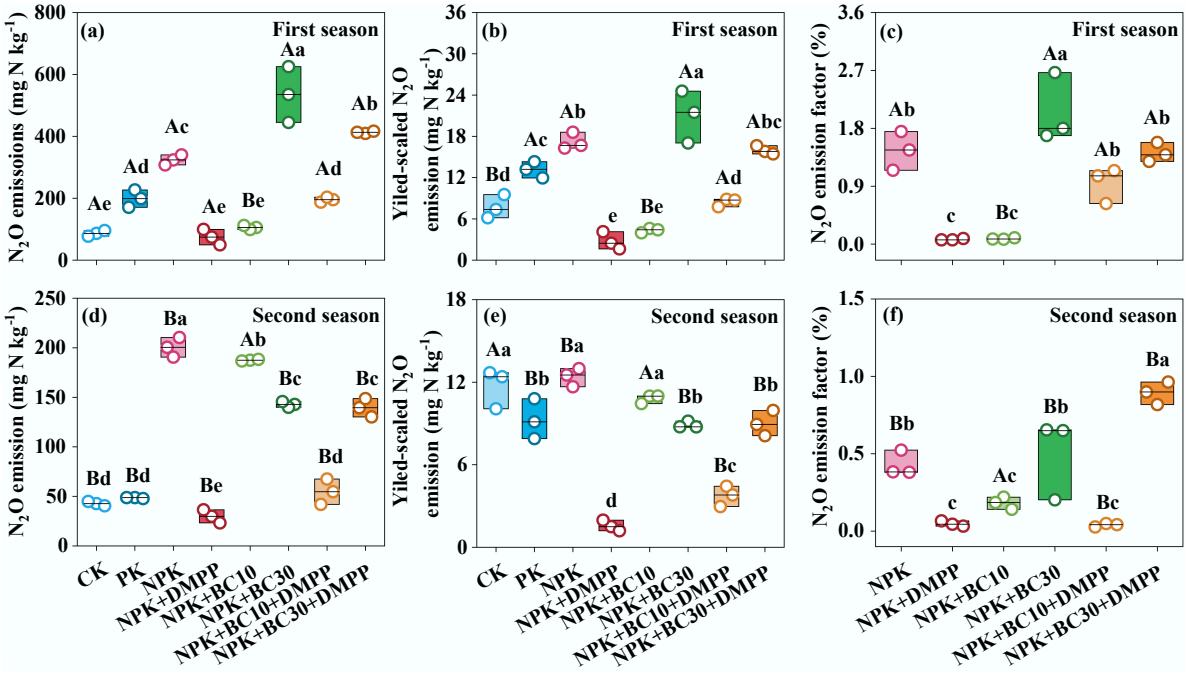

Fig. 2 Changes in (**a**), (**d**) cumulative N_2O emission, (**b**), (**e**) yield-scaled N_2O emission, and (**c**), (**f**) N_2O emission factor after fertilizer application during the first and second seasons. Different lowercase and uppercase letters indicate significant differences between fertilization treatments and growing seasons, respectively. The absence of letters indicates no significant differences. The values represent the average ± standard deviation ($n = 3$).

observed in the second season. Similarly, N_2O emissions under NPK + BC10 + DMPP were significantly lower than those under NPK + BC30 + DMPP across both seasons. Both NPK + DMPP and NPK + BC10 + DMPP significantly reduced yield-scaled N_2O emissions in both seasons, with NPK + DMPP showing the greatest reduction. Furthermore, both NPK + DMPP and NPK + BC10 significantly decreased N_2O emission factors in both seasons.

Soil inorganic N supply and immobilization rates, N residence time, and N-cycling functional gene abundances

Soil inorganic N supply, immobilization rates, and N residence times were strongly influenced by fertilization treatments, growing seasons, and their interactions (Figs 3 & 4). The gross N mineralization rate varied from 2.35 to 8.32 mg N kg^{-1} d^{-1}. NPK + BC10 and NPK + BC30 significantly enhanced gross N mineralization rate in the first season, whereas NPK + DMPP significantly decreased it in the second season. Across both seasons, NPK + BC30 consistently exhibited greater gross N mineralization rates than NPK + DMPP. Gross NH_4^+ immobilization rates ranged from 5.28 to 15.3 mg N kg^{-1} d^{-1}. NPK + DMPP significantly reduced gross NH_4^+ immobilization rates in both seasons (5.28 and 7.62 mg N kg^{-1} d^{-1}), with values considerably lower than those observed under all biochar-containing treatments.

Gross nitrification rates varied from 6.89 to 18.3 mg N kg^{-1} d^{-1}. NPK + DMPP (6.89 and 8.57 mg N kg^{-1} d^{-1}) and NPK + BC10 + DMPP (13.7 and 13.0 mg N kg^{-1} d^{-1}) significantly reduced nitrification rates in both seasons, with NPK + DMPP showing the most potent inhibition. The nitrification rate under NPK + DMPP remained consistently lower than under all biochar-related treatments in both seasons. Gross NO_3^- immobilization rates varied from 3.20 to 9.82 mg N kg^{-1} d^{-1}. NPK + DMPP significantly reduced gross NO_3^- immobilization to 3.21 and 4.31 mg N kg^{-1} d^{-1} in both seasons, with values significantly lower than those under all biochar-containing treatments. The total gross immobilization rate was lowest under NPK + DMPP across both seasons (8.48 and 11.9 mg N kg^{-1} d^{-1}). The ratio of gross NH_4^+ immobilization to gross nitrification (GAI/GN) remained consistently below 1 for all treatments. NPK + DMPP exhibited the highest GAI/GN ratio in both seasons, significantly exceeding those under NPK + BC10, NPK + BC30, and NPK + BC30 + DMPP in the first season. NPK + DMPP also resulted in the longest NH_4^+ residence times (1.70 and 1.19 d) and NO_3^- residence times (0.94 and 1.78 d) in both seasons, significantly longer than under NPK + BC30 and NPK + BC30 + DMPP.

Fertilization treatments, growing seasons, and their interactions also significantly affected AOA and AOB abundances. In the first season, AOA abundance under NPK + DMPP was greatly lower than under all biochar-containing treatments. In the second season, AOA abundance under NPK + BC10 was significantly lower than under NPK + BC10 + DMPP and NPK + BC30 + DMPP. AOB abundance under NPK + DMPP was significantly lower than under NPK + BC30 and NPK + BC30 + DMPP in both seasons. Similarly, AOB abundance under NPK + BC10 was significantly lower than under DPK + BC30 and NPK + BC30 + DMPP in both seasons.

Relationships among crop yield, NUE, soil properties, inorganic N turnover rates, functional gene abundances, and N_2O emissions

Across both seasons, crop yield showed a significant positive correlation with the gross NH_4^+ immobilization-to-nitrification ratio and the mean NH_4^+ residence time (Fig. 5). Similarly, NUE also exhibited a strong positive correlation with mean NH_4^+ residence time across both seasons. Soil N_2O emissions were significantly and positively related to soil pH and gross nitrification rates in both seasons. Across both seasons, the gross N mineralization rate was positively

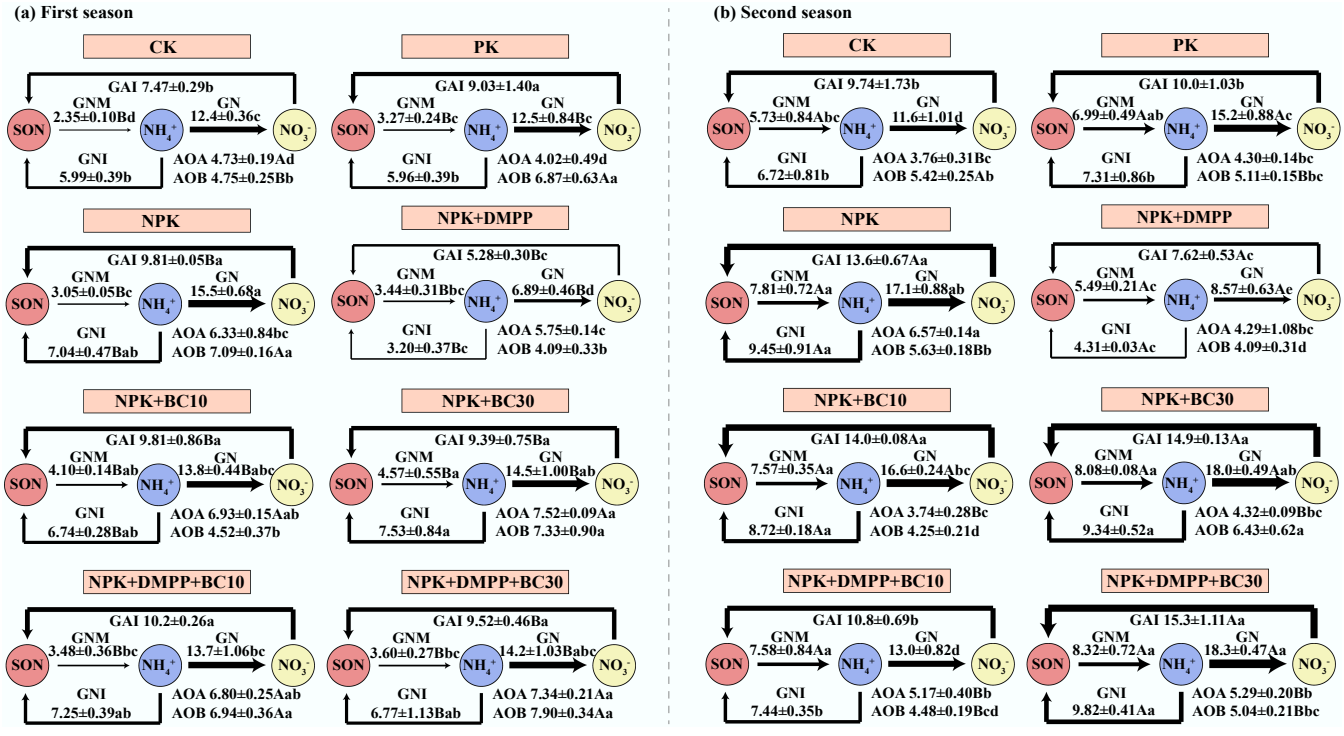

Fig. 3 Changes in soil inorganic N supply, microbial immobilization rates, and N cycling functional gene abundances after fertilizer application during the first and second seasons. All N-cycling functional gene abundances were log-transformed. Different lowercase and uppercase letters indicate significant differences between fertilization treatments and growing seasons, respectively. The absence of letters indicates no significant differences. The values represent the average ± standard deviation (n = 3).

https://doi.org/10.48130/nc-0025-0013

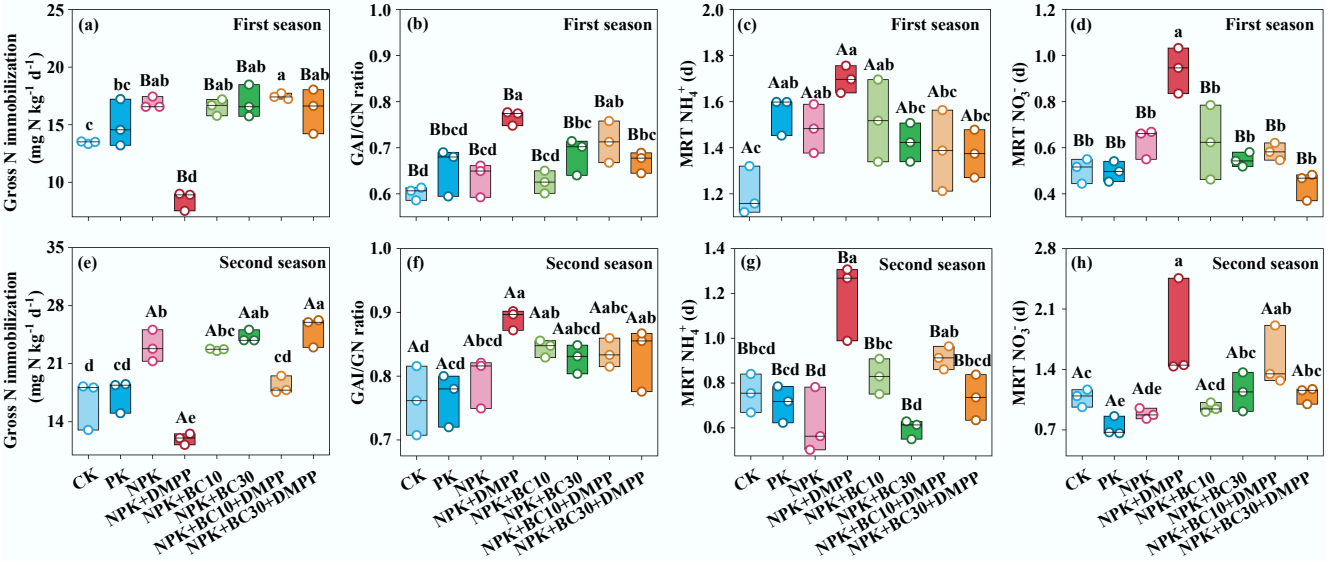

Fig. 4 Changes in (**a**), (**e**) gross N immobilization, (**b**), (**f**) gross NH_4^+ immobilization/gross nitrification (GAI/GN) ratio, (**c**), (**g**) mean residence time of NH_4^+ (MRT NH_4^+), and (**d**), (**h**) mean residence time of NO_3^- (MRT NO_3^-) after fertilizer application during the first and second seasons. Different lowercase and uppercase letters indicate significant differences between fertilization treatments and growing seasons, respectively. The absence of letters indicates no significant differences. The values represent the average ± standard deviation (n = 3).

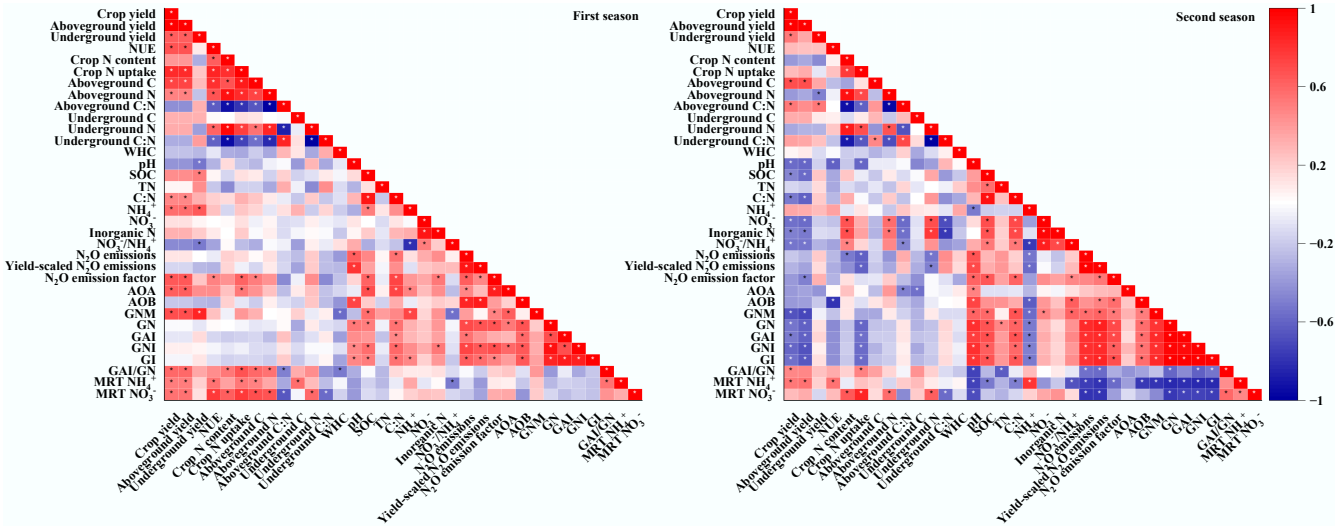

Fig. 5 Relationships between crop yields, crop nutrient contents, soil physicochemical and microbial properties, inorganic N supply and immobilization rates, and soil N_2O emissions. WHC, water holding capacity; SOC, soil organic C; TN, total N; GNM, gross N mineralization; GN, gross nitrification; GAI, gross NH_4^+ immobilization; GNI, gross NO_3^- immobilization; GI, gross immobilization; MRT NH_4^+, mean residence time of NH_4^+; MRT NO_3^-, mean residence time of NO_3^-. * indicates $p < 0.05$.

associated with soil organic C. In contrast, the gross nitrification rate was positively correlated with soil pH, organic C, and AOB abundance.

Discussion

DMPP outperformed biochar in enhancing crop yield, NUE, and mitigating N_2O emissions

The present results indicate that both biochar and DMPP, whether applied alone or in combination, enhanced crop yield to varying degrees, although the magnitude of these effects differed significantly between seasons. This enhancement was primarily attributed to the capacity of biochar and/or DMPP to promote soil inorganic N retention, thereby facilitating crop N uptake and utilization[33,34]. However, in calcareous soils, DMPP application alone exhibited the most pronounced and consistent benefits, resulting in the highest crop N uptake, yield, and NUE, while simultaneously generating the lowest soil N_2O emissions across both seasons. This superior performance of DMPP is closely linked to the inherently high pH of calcareous soils. DMPP primarily inhibits ammonia oxidation, an effect known to be particularly effective under alkaline conditions[48,49], thereby delaying the oxidation of NH_4^+ to NO_3^- and prolonging NH_4^+ residence time in soil[26,34]. This mechanism increases N availability in the rhizosphere while reducing NO_3^- leaching and denitrification losses[37,50]. This observation aligns with numerous studies demonstrating that DMPP effectively decreases N leaching and N_2O emissions in alkaline soils[51,52]. Moreover, our study further revealed that nitrification was the dominant pathway of N_2O production in calcareous soils, as

evidenced by the 77.0%–85.1% reduction in N_2O emissions following DMPP application relative to NPK alone. Previous studies have shown that nitrification can be effectively inhibited at relatively low DMPP doses in alkaline soils, whereas higher doses are required in acidic soils[49]. Beyond influencing DMPP bioavailability, soil pH can regulate the composition and activity of nitrifying microbial communities through niche specialization[11,37,49]. Consequently, the present results indicate that DMPP enhances crop N uptake and utilization while simultaneously suppressing N_2O production, making it a promising management strategy for achieving high NUE and mitigating greenhouse gas emissions in calcareous soils.

These findings partially contradict our hypothesis that combining DMPP with biochar would synergistically enhance crop yield. Instead, DMPP alone outperformed both biochar application alone and their combination. This may be attributed to the contrasting mechanisms of the two amendments and their antagonistic interactions in alkaline soil conditions[51,53]. Biochar, rich in labile C and characterized by a well-developed porous structure, can increase soil C availability and improve aeration[54], potentially stimulating both nitrification and denitrification processes[55]. In soils where nitrification is the primary source of N_2O, biochar has been reported to increase N_2O emissions relative to DMPP alone[55,56], as biochar may promote the complete denitrification in alkaline soils by facilitating electron transfer to denitrifying microbes and enhancing the abundance of N_2O-reducing bacteria[57,58]. Meanwhile, the increased NO_3^- production in biochar-amended soil also poses high N leaching losses potential[10,52,59], although there are currently no direct comparative evaluations between biochar and DMPP in calcareous soils. Moreover, the abundant acidic functional groups such as carboxyl (-COOH) and hydroxyl (-OH) on biochar surfaces impart a strong negative charge[31,60], which facilitates the adsorption of positively charged DMPP molecules[61,62]. Such adsorption may reduce the effective DMPP concentration in the soil solution, thereby weakening its inhibitory effect on AMO activity[37,43]. Consequently, biochar application did not enhance—but rather partially offset—the inhibitory effects of DMPP, leading to increased N_2O emissions, reduced crop N uptake and NUE, and ultimately limiting further yield improvement. Furthermore, the biochar application rate significantly influenced crop N uptake and yield. Although high biochar (30 t ha^{-1}) application increased crop N uptake and N content, its contribution to yield improvement was limited and even declined in the second season. This may be associated with the reduced NUE and higher N_2O emission factor observed under high biochar application. The significant increase in soil organic C resulting from high biochar application favors inorganic N supply and enhances denitrification potential, thereby increasing N_2O emissions and NO_3^- losses risks, which in turn impairs NUE and constrains yield improvement[55]. Additionally, some studies have shown that high biochar may reduce NO_3^- leaching in alkaline soils via adsorption and enhanced water retention[59] or exert minimal influence on N leaching[63], highlighting that the relative severity of N losses under biochar vs DMPP requires further empirical verification.

DMPP outperformed biochar in reducing nitrification and enhancing inorganic N retention

The residence times of NH_4^+ and NO_3^- in soil depend on the dynamic balance among multiple N transformation processes, including production (e.g., mineralization and nitrification) and consumption (e.g., immobilization, leaching, and gaseous losses), which collectively influence the dominant inorganic N forms, their fate, and availability[22,64]. Our results showed that DMPP application alone significantly prolonged the residence times of both NH_4^+ and NO_3^- in soil across both seasons, and NH_4^+ residence time was positively correlated with crop yield and NUE (Figs 4 & 5). This indicates that DMPP can enhance N retention by delaying the rapid conversion of NH_4^+, thereby improving NUE and increasing crop yield. Indeed, DMPP application alone significantly reduced gross nitrification rates in both seasons and inhibited gross N mineralization only in the second season, supporting its positive effect in prolonging NH_4^+ residence time in calcareous soils. As a copper-chelating nitrification inhibitor, DMPP binds to copper ions at the active sites of AMO enzymes used by ammonia-oxidizing microorganisms (AOB and AOA), thereby reducing AMO activity and directly inhibiting the nitrification rate[26,34]. In this study, DMPP significantly decreased AOB abundance in both seasons. At the same time, its inhibitory effect on AOA was significant only in the second season, indicating that AOB played a dominant role in DMPP-induced reduction of the nitrification rate in calcareous soils. This is in line with previous studies[11,37], which have shown that AOB typically dominate nitrification under high-N, neutral, or slightly alkaline conditions. In contrast, AOA are more competitive in low-N or acidic soils. Therefore, the present results indicate that the differential reactivity of DMPP under different pH regimes is closely related to the distinct pH sensitivities of AOB and AOA. By inhibiting AOB activity, DMPP not only extended NH_4^+ residence time but also reduced NO_3^- availability, thereby lowering the substrate supply for denitrification and ultimately reducing N_2O emissions[65–67]. The significant positive correlations observed among AOB abundances, gross nitrification rates, and N_2O emissions further confirm that nitrification was the primary source of N_2O in these calcareous soils. In addition, some studies have suggested that because NO_3^- and N_2O compete as electron acceptors during denitrification, lower NO_3^- concentrations may increase the N_2/N_2O ratio, promoting complete reduction to N_2 and thereby reducing N_2O emissions[67,68].

In contrast, compared to DMPP alone, both low (10 t ha^{-1}) and high (30 t ha^{-1}) biochar application rates significantly enhanced microbial NH_4^+ and NO_3^- immobilization rates but shortened their residence times, indicating that the impacts of biochar on soil inorganic N supply and retention are more complex. Compared to DMPP alone, biochar addition significantly enhanced gross N mineralization and nitrification rates, although the magnitude of stimulation varied with biochar application rate and season. Soil pH and organic C content are key factors driving both gross N mineralization and nitrification rates[22,69]. In the present study, biochar application (at both 10 and 30 t ha^{-1}) showed significantly higher soil pH and organic C contents than DMPP alone, both of which were positively associated with gross N mineralization and nitrification rates, indicating that biochar indirectly stimulates these processes by enhancing soil energy supply and modifying microbial metabolic environments. As gross N mineralization increased, greater NH_4^+ availability provided more substrate for nitrification rather than microbial assimilation, indicating that higher substrate supply further stimulated nitrification. This was supported by the lower GAI/GN ratio observed under biochar treatments. Moreover, the well-developed porous structure of biochar can improve soil aeration, creating favorable aerobic conditions for ammonia-oxidizing microorganisms (AOA and AOB), thereby potentially increasing nitrification rates[70,71]. The increased inorganic N supply subsequently stimulated microbial immobilization of NH_4^+ and NO_3^-. The above effects were more pronounced at higher biochar application rates (30 t ha^{-1}). Furthermore, the present results found that biochar application, whether alone or combined with DMPP, consistently increased N_2O emissions. This could be because organic C sources serve as electron donors for denitrifiers, and greater C availability generally stimulates denitrification and increases N_2O emissions[72,73]. The elevated C inputs from biochar likely accelerated C mineralization and microbial respiration, which, in turn,

increased oxygen consumption and promoted the formation of anoxic microenvironments, supporting higher denitrified abundances and favoring denitrification, particularly under high soil pH and sufficient NO_3^- supply[74]. This mechanism likely contributes to the positive correlations observed between soil organic C content, pH, and N_2O emissions in the present study (Supplementary Fig. S3). Growing evidence further suggested that a substantial portion of labile C released from biochar may directly fuel denitrification[75]. For example, Lan et al.[74] found that liable C significantly enhanced denitrification rate, N_2O emissions, and the $N_2O/(N_2O + N_2)$ ratio by upregulating *nirK* and *nirS* genes in calcareous soil. Similarly, Surey et al.[75] also reported that denitrification in Haplic Chernozem soils (pH 6.9–7.4) is strongly driven by labile organic matter, and that high C bioavailability triggers incomplete denitrification, resulting in higher N_2O/N_2 ratios. In addition to providing more favorable soil physiochemical conditions, greater substrate and energy availability, the abundant surface functional groups and extensive pore network of biochar may also create physical niches and spatial separation for nitrifying and denitrifying microorganisms[31,76]. This may permit microzones with contrasting redox conditions to coexist, facilitate rapid substrate exchange, and promote the accumulation of N_2O as an intermediate product[55,76]. Noticeably, the strong adsorption capacity of biochar for DMPP molecules may lower their effective concentration in soil solution, thereby weakening DMPP's inhibitory effect on AMO activity[61,62]. This could explain the observed increases in nitrification rate and N_2O emissions under co-application of biochar and DMPP.

Overall, DMPP achieved superior NUE enhancement and stronger N_2O emission mitigation by directly inhibiting ammonia-oxidizing microorganisms, suppressing nitrification, and prolonging inorganic N retention in soil. In contrast, although biochar improved soil physicochemical properties, its effects were highly dependent on application rate, growing season, and its interaction with DMPP. Therefore, in calcareous soils, an N management strategy centered on DMPP should be prioritized. By optimizing biochar application rates and combining it with DMPP, it is possible to simultaneously maximize NUE and mitigate greenhouse gas emissions, thereby improving both productivity and environmental sustainability in calcareous agroecosystems. Nonetheless, further investigation into plant N uptake pathways, denitrifier functional genes, denitrification dynamics, and N leaching losses are needed to more fully assess the relative effects of DMPP and biochar on soil N fate and NUE.

Conclusions

DMPP application alone greatly improved crop N uptake, NUE, and yield in both seasons while simultaneously decreasing soil N_2O emissions, highlighting its superior potential to enhance NUE in calcareous soils. The primary mechanism is that DMPP suppresses AOB activity and decreases soil nitrification rates, thereby increasing microbial NH_4^+ immobilization-to-nitrification ratio, extending the residence time of NH_4^+ and NO_3^- in soil, reducing N_2O production, and enhancing N retention and utilization efficiency. In contrast, biochar applied at 10 and 30 t ha^{-1} promoted microbial assimilation of inorganic N but significantly increased nitrification rates and shortened the residence time of inorganic N, ultimately resulting in lower NUE and higher N_2O emissions. Even when co-applied with DMPP, these adverse effects were not substantially alleviated. Overall, DMPP proved more effective than biochar in retaining inorganic N, promoting crop yield, improving NUE, and substantially mitigating N_2O emissions in calcareous soils. Therefore, DMPP should be prioritized as the core N fertilizer management strategy in calcareous croplands, while moderate adjustment of biochar application rates and ratios may help achieve synergistic improvements in both agronomic productivity and environmental sustainability.

Supplementary information

It accompanies this paper at: https://doi.org/10.48130/nc-0025-0013.

Author contributions

The authors confirm their contributions to the paper as follows: Lijun Liu: data collection, data analysis, and writing–draft manuscript preparation; Nana Ding: material preparation, data collection, and data analysis; Lei Meng: study design; Tongbin Zhu: conceptualization, study design, funding acquisition, supervision, and writing–review and editing; Qi Xu: material preparation; Ahmed S. Elrys: data analysis; Lee Kheng Heng: data analysis; Christoph Müller: data collection. All authors reviewed the results and approved the final version of the manuscript.

Data availability

The data that support the findings of this study are available upon request from the corresponding author.

Funding

This research was supported by the Key R&D Programs of Guangxi (Grant No. Guikenong AB241484038), the Guangxi Science and Technology Planning Project (Grant No. 2023GXNSFFA026010), the CAGS Research Fund (Grant No. YYWF 2023015), and the Geological Survey Project, China (Grant No. DD20240095).

Declarations

Competing interests

The authors declare that they have no known competing financial interests or personal relationships that could have appeared to influence the work reported in this paper.

Author details

[1]Institute of Karst Geology, CAGS/Key Laboratory of Karst Dynamics, MNR & GZAR/International Research Center on Karst under the Auspices of UNESCO, Guilin, Guangxi 541004, China; [2]Pingguo Guangxi, Karst Ecosystem, National Observation and Research Station, Pingguo, Guangxi 531406, China; [3]Institute of Plant Ecology, Justus–Liebig University Giessen, Heinrich–Buff–Ring 26, Giessen 35392, Germany; [4]School of Breeding and Multiplication (Sanya Institute of Breeding and Multiplication), Hainan University, Sanya, Hainan 572025, China; [5]College of Agriculture, University of Al Dhaid, Al Dhaid, Sharja, United Arab Emirates; [6]School of Tropical Agriculture and Forest, Hainan University, Haikou 570228, China; [7]International Atomic Energy Agency, Vienna 1400, Austria; [8]School of Biology and Environmental Science and Earth Science Centre, University College Dublin, Belfield, Dublin 4, Ireland

References

[1] Lentz RD, Ippolito JA, Spokas KA. 2014. Biochar and manure effects on net nitrogen mineralization and greenhouse gas emissions from calcareous soil under corn. *Soil Science Society of America Journal* 78:1641–1655

[2] Amin AEEAZ, Eissa MA. 2017. Biochar effects on nitrogen and phosphorus use efficiencies of zucchini plants grown in a calcareous sandy soil. *Journal of Soil Science and Plant Nutrition* 17:912–921

[3] Wang X, Liu X, Wang W. 2022. National-scale distribution and its influence factors of calcium concentrations in Chinese soils from the China Global Baselines project. *Journal of Geochemical Exploration* 233:106907

[4] Ortiz C, Pierotti S, Molina MG, Bosch-Serra ÀD. 2023. Soil fertility and phosphorus leaching in irrigated calcareous soils of the Mediterranean Region. *Environmental Monitoring and Assessment* 195:1376

[5] Sarker RR, Rashid MH, Islam MA, Jahiruddin M, Islam KR, et al. 2023. Tillage and residue management impact on microbial and nematode abundance under diverse rice-based cropping systems in calcareous and non-calcareous floodplain soils. *Journal of Soil Science and Plant Nutrition* 23:2138–2151

[6] Zahedifard N, Shahbazi K, Mohammadi MH, Golchin A, Moshiri F, et al. 2024. Soil organic carbon fractions in cultivated calcareous soils. *Eurasian Soil Science* 57:780–793

[7] Long X, Li J, Liao X, Wang J, Zhang W, et al. 2025. Stable soil biota network enhances soil multifunctionality in agroecosystems. *Global Change Biology* 31:e70041

[8] Chen X, Zhang Z. 2022. An overview on the development of science and ecological hydrology of the earth critical zones in karst area. *Carsologica Sinica* 41:356–364 (in Chinese)

[9] Liu X, Li SL, Yue FJ, Zhong J, Qin CQ, et al. 2022. Biogeochemical cycles of karst systems and their response to global change. *Carsologica Sinica* 41:465–476 (in Chinese)

[10] Lan T, Huang Y, Song X, Deng O, Zhou W, et al. 2022. Biological nitrification inhibitor co-application with urease inhibitor or biochar yield different synergistic interaction effects on NH_3 volatilization, N leaching, and N use efficiency in a calcareous soil under rice cropping. *Environmental Pollution* 293:118499

[11] Zou W, Lang M, Zhang L, Liu B, Chen X. 2022. Ammonia-oxidizing bacteria rather than ammonia-oxidizing archaea dominate nitrification in a nitrogen-fertilized calcareous soil. *Science of The Total Environment* 811:151402

[12] Zhu T, Zeng S, Qin H, Zhou K, Yang H, et al. 2016. Low nitrate retention capacity in calcareous soil under woodland in the karst region of southwestern China. *Soil Biology and Biochemistry* 97:99–101

[13] Garousi F, Shan Z, Ni K, Yang H, Shan J, et al. 2021. Decreased inorganic N supply capacity and turnover in calcareous soil under degraded rubber plantation in the tropical karst region. *Geoderma* 381:114754

[14] Li D, Yang Y, Chen H, Xiao K, Song T, et al. 2017. Soil gross nitrogen transformations in typical karst and nonkarst forests, southwest China. *Journal of Geophysical Research: Biogeosciences* 122:2831–2840

[15] Adalibieke W, Cui X, Cai H, You L, Zhou F. 2023. Global crop-specific nitrogen fertilization dataset in 1961–2020. *Scientific Data* 10:617

[16] Martre P, Dueri S, Guarin JR, Ewert F, Webber H, et al. 2024. Global needs for nitrogen fertilizer to improve wheat yield under climate change. *Nature Plants* 10:1081–1090

[17] Pramanick B, Choudhary S, Kumar M, Singh SK, Jha RK, et al. 2024. Can site-specific nutrient management improve the productivity and resource use efficiency of climate-resilient finger millet in calcareous soils in India? *Heliyon* 10:e32774

[18] Rashid M, Hussain Q, Khan KS, Ali Alvi S, Abro SA, et al. 2025. De-ashed-biochar slow-release N fertilizer increased NUE in alkaline calcareous soils under wheat and maize crops. *Scientific Reports* 15:7748

[19] You L, Ros GH, Chen Y, Zhang F, de Vries W. 2024. Optimized agricultural management reduces global cropland nitrogen losses to air and water. *Nature Food* 5:995–1004

[20] You L, Ros GH, Chen Y, Shao Q, Young M, et al. 2023. Global mean nitrogen recovery efficiency in croplands can be enhanced by optimal nutrient, crop and soil management practices. *Nature Communications* 14:5747

[21] Qayyum MF, Abdullah MA, Rizwan M, Haider G, Ali MA, et al. 2019. Different nitrogen and biochar sources' application in an alkaline calcareous soil improved the maize yield and soil nitrogen retention. *Arabian Journal of Geosciences* 12:664

[22] Elrys AS, Wang J, Meng L, Zhu Q, El-Sawy MM, et al. 2023. Integrative knowledge-based nitrogen management practices can provide positive effects on ecosystem nitrogen retention. *Nature Food* 4:1075–1089

[23] Grandy AS, Daly AB, Bécu T, Cardinael R, Fontaine S, et al. 2024. A microbial framework for nitrogen cycling solutions in agroecosystems. *One Earth* 7:2103–2107

[24] Sheikhi J, Mirsyed Hosseini H, Etesami H, Majidi A. 2024. Biochar versus crop residues: modulating net nitrogen mineralization-immobilization and lowering nitrification in calcareous soils. *Journal of Soil Science and Plant Nutrition* 24:231–251

[25] Aamer M, Shaaban M, Hassan MU, Huang G, Liu Y, et al. 2020. Biochar mitigates the N_2O emissions from acidic soil by increasing the *nosZ* and *nirK* gene abundance and soil pH. *Journal of Environmental Management* 255:109891

[26] Beeckman F, Annetta L, Corrochano-Monsalve M, Beeckman T, Motte H. 2024. Enhancing agroecosystem nitrogen management: microbial insights for improved nitrification inhibition. *Trends in Microbiology* 32:590–601

[27] Gezahegn A, Selassie YG, Agegnehu G, Addisu S, Mihretie FA, et al. 2025. Synergistic effects of aquatic weed biochar and inorganic fertilizer on soil properties, maize yield, and nitrogen use efficiency on Nitisols of Northwestern Ethiopian Highlands. *Journal of Agriculture and Food Research* 21:101939

[28] Saffari N, Hajabbasi MA, Shirani H, Mosaddeghi MR, Mamedov AI. 2020. Biochar type and pyrolysis temperature effects on soil quality indicators and structural stability. *Journal of Environmental Management* 261:110190

[29] Zhang L, Jing Y, Chen C, Xiang Y, Rezaei Rashti M, et al. 2021. Effects of biochar application on soil nitrogen transformation, microbial functional genes, enzyme activity, and plant nitrogen uptake: a meta-analysis of field studies. *Global Change Biology Bioenergy* 13:1859–1873

[30] Ullah MS, Malekian R, Randhawa GS, Gill YS, Singh S, et al. 2024. The potential of biochar incorporation into agricultural soils to promote sustainable agriculture: insights from soil health, crop productivity, greenhouse gas emission mitigation and feasibility perspectives—a critical review. *Reviews in Environmental Science and Bio/Technology* 23:1105–1130

[31] Clough TJ, Condron LM. 2010. Biochar and the nitrogen cycle: introduction. *Journal of Environmental Quality* 39:1218–1223

[32] Wang Z, Zong H, Zheng H, Liu G, Chen L, et al. 2015. Reduced nitrification and abundance of ammonia-oxidizing bacteria in acidic soil amended with biochar. *Chemosphere* 138:576–583

[33] Guo C, Wang H, Zou D, Wang Y, Han X. 2022. A novel amended nitrification inhibitor confers an enhanced suppression role in the nitrification of ammonium in soil. *Journal of Soils and Sediments* 22:831–843

[34] Tufail MA, Irfan M, Umar W, Wakeel A, Schmitz RA. 2023. Mediation of gaseous emissions and improving plant productivity by DCD and DMPP nitrification inhibitors: meta-analysis of last three decades. *Environmental Science and Pollution Research* 30:64719–64735

[35] Weiske A, Benckiser G, Herbert T, Ottow J. 2001. Influence of the nitrification inhibitor 3,4-dimethylpyrazole phosphate (DMPP) in comparison to dicyandiamide (DCD) on nitrous oxide emissions, carbon dioxide fluxes and methane oxidation during 3 years of repeated application in field experiments. *Biology and Fertility of Soils* 34:109–117

[36] Ruser R, Schulz R. 2015. The effect of nitrification inhibitors on the nitrous oxide (N_2O) release from agricultural soils—a review. *Journal of Plant Nutrition and Soil Science* 178:171–188

[37] Li J, Wang S, Luo J, Zhang L, Wu Z, et al. 2021. Effects of biochar and 3,4-dimethylpyrazole phosphate (DMPP) on soil ammonia-oxidizing bacteria and *nosZ*-N_2O reducers in the mitigation of N_2O emissions from paddy soils. *Journal of Soils and Sediments* 21:1089–1098

[38] Li Z, Xu P, Han Z, Wu J, Bo X, et al. 2023. Effect of biochar and DMPP application alone or in combination on nitrous oxide emissions differed by soil types. *Biology and Fertility of Soils* 59:123–138

[39] He X, He J, Shen H, Zeng Z, Zhao D, et al. 2025. Co-application of nitrification inhibitors with straw or biochar yielded varying effects on soil nitrification rate, N_2O emissions, and ammonia oxidizers. *Journal of Soils and Sediments* 25:1949–1961

[40] Fu Q, Yan J, Li H, Li T, Hou R, et al. 2019. Effects of biochar amendment on nitrogen mineralization in black soil with different moisture contents under freeze-thaw cycles. *Geoderma* 353:459–467

[41] Hu T, Wei J, Du L, Chen J, Zhang J. 2023. The effect of biochar on nitrogen availability and bacterial community in farmland. *Annals of Microbiology* 73:4
[42] Abujabhah IS, Doyle R, Bound SA, Bowman JP. 2016. The effect of biochar loading rates on soil fertility, soil biomass, potential nitrification, and soil community metabolic profiles in three different soils. *Journal of Soils and Sediments* 16:2211−2222
[43] Fuertes-Mendizábal T, Huérfano X, Vega-Mas I, Torralbo F, Menéndez S, et al. 2019. Biochar reduces the efficiency of nitrification inhibitor 3,4-dimethylpyrazole phosphate (DMPP) mitigating N_2O emissions. *Scientific Reports* 9:2346
[44] Priha O, Smolander A. 1999. Nitrogen transformations in soil under *Pinus sylvestris*, *Picea abies* and *Betula pendula* at two forest sites. *Soil Biology and Biochemistry* 31:965−977
[45] Bremner JM, Keeney DR. 1966. Determination and isotope-ratio analysis of different forms of nitrogen in soils: 3. exchangeable ammonium, nitrate, and nitrite by extraction-distillation methods. *Soil Science Society of America Journal* 30:577−582
[46] Kirkham D, Bartholomew WV. 1954. Equations for following nutrient transformations in soil, utilizing tracer data. *Soil Science Society of America Journal* 18:33−34
[47] Corre MD, Brumme R, Veldkamp E, Beese FO. 2007. Changes in nitrogen cycling and retention processes in soils under spruce forests along a nitrogen enrichment gradient in Germany. *Global Change Biology* 13:1509−1527
[48] Li S, Sha Z, Xu B, Gui D, Yang Q. 2025. Nitrification inhibition lowers inorganic carbon-induced CO_2 loss and impedes N_2O emissions from three calcareous soils. *Plant and Soil* 2025:1−21
[49] Bachtsevani E, Papazlatani CV, Rousidou C, Lampronikou E, Menkissoglu-Spiroudi U, et al. 2021. Effects of the nitrification inhibitor 3,4-dimethylpyrazole phosphate (DMPP) on the activity and diversity of the soil microbial community under contrasting soil pH. *Biology and Fertility of Soils* 57:1117−1135
[50] Barrena I, Menéndez S, Correa-Galeote D, Vega-Mas I, Bedmar EJ, et al. 2017. Soil water content modulates the effect of the nitrification inhibitor 3,4-dimethylpyrazole phosphate (DMPP) on nitrifying and denitrifying bacteria. *Geoderma* 303:1−8
[51] Chen H, Yin C, Fan XP, Ye MJ, Peng HY, et al. 2019. Reduction of N_2O emission by biochar and/or 3,4-dimethylpyrazole phosphate (DMPP) is closely linked to soil ammonia oxidizing bacteria and nosZI-N_2O reducer populations. *Science of The Total Environment* 694:133658
[52] Guo B, Zheng X, Yu J, Ding H, Luo S, et al. 2022. Liming and nitrification inhibitor affects crop N uptake efficiency and N loss through changing soil N processes. *Biology and Fertility of Soils* 58:949−959
[53] Keiblinger KM, Zehetner F, Mentler A, Zechmeister-Boltenstern S. 2018. Biochar application increases sorption of nitrification inhibitor 3,4-dimethylpyrazole phosphate in soil. *Environmental Science and Pollution Research* 25:11173−11177
[54] Chagas JKM, Figueiredo CCD, Ramos MLG. 2022. Biochar increases soil carbon pools: evidence from a global meta-analysis. *Journal of Environmental Management* 305:114403
[55] Sánchez-García M, Roig A, Sánchez-Monederoonedero MA, Cayuela ML. 2014. Biochar increases soil N_2O emissions produced by nitrification-mediated pathways. *Frontiers in Environmental Science* 2:25
[56] Wells NS, Baggs EM. 2014. Char amendments impact soil nitrous oxide production during ammonia oxidation. *Soil Science Society of America Journal* 78:1656−1660
[57] Liu Q, Zhang Y, Liu B, Amonette JE, Lin Z, et al. 2018. How does biochar influence soil N cycle? A meta-analysis. *Plant and Soil* 426:211−225
[58] Liu Q, Liu B, Zhang Y, Hu T, Lin Z, et al. 2019. Biochar application as a tool to decrease soil nitrogen losses (NH_3 volatilization, N_2O emissions, and N leaching) from croplands: options and mitigation strength in a global perspective. *Global Change Biology* 25:2077−2093
[59] Lan T, He X, Wang Q, Deng O, Zhou W, et al. 2022. Synergistic effects of biological nitrification inhibitor, urease inhibitor, and biochar on NH_3 volatilization, N leaching, and nitrogen use efficiency in a calcareous soil–wheat system. *Applied Soil Ecology* 174:104412
[60] Wang J, Wang S. 2019. Preparation, modification and environmental application of biochar: a review. *Journal of Cleaner Production* 227:1002−1022
[61] Marsden KA, Marín-Martínez AJ, Vallejo A, Hill PW, Jones DL, et al. 2016. The mobility of nitrification inhibitors under simulated ruminant urine deposition and rainfall: a comparison between DCD and DMPP. *Biology and Fertility of Soils* 52:491−503
[62] Guardia G, Marsden KA, Vallejo A, Jones DL, Chadwick DR. 2018. Determining the influence of environmental and edaphic factors on the fate of the nitrification inhibitors DCD and DMPP in soil. *Science of The Total Environment* 624:1202−1212
[63] Sun H, Lu H, Chu L, Shao H, Shi W. 2017. Biochar applied with appropriate rates can reduce N leaching, keep N retention and not increase NH_3 volatilization in a coastal saline soil. *Science of The Total Environment* 575:820−825
[64] Kuypers MMM, Marchant HK, Kartal B. 2018. The microbial nitrogen-cycling network. *Nature Reviews Microbiology* 16:263−276
[65] Cassman NA, Soares JR, Pijl A, Lourenço KS, Van Veen JA, et al. 2019. Nitrification inhibitors effectively target N_2O-producing *Nitrosospira* spp. in tropical soil. *Environmental Microbiology* 21:1241−1254
[66] Han B, Yao Y, Liu B, Wang Y, Su X, et al. 2024. Relative importance between nitrification and denitrification to N_2O from a global perspective. *Global Change Biology* 30:e17082
[67] Prosser JI, Hink L, Gubry-Rangin C, Nicol GW. 2020. Nitrous oxide production by ammonia oxidizers: physiological diversity, niche differentiation and potential mitigation strategies. *Global Change Biology* 26:103−118
[68] Ruser R, Flessa H, Russow R, Schmidt G, Buegger F, et al. 2006. Emission of N_2O, N_2 and CO_2 from soil fertilized with nitrate: effect of compaction, soil moisture and rewetting. *Soil Biology and Biochemistry* 38:263−274
[69] Elrys AS, Ali A, Zhang H, Cheng Y, Zhang J, et al. 2021. Patterns and drivers of global gross nitrogen mineralization in soils. *Global Change Biology* 27:5950−5962
[70] Pokharel P, Qi L, Chang SX. 2021. Manure-based biochar decreases heterotrophic respiration and increases gross nitrification rates in rhizosphere soil. *Soil Biology and Biochemistry* 154:108147
[71] Hale L, Hendratna A, Scott N, Gao S. 2023. Biochar enhancement of nitrification processes varies with soil conditions. *Science of The Total Environment* 887:164146
[72] Cayuela ML, Van Zwieten L, Singh BP, Jeffery S, Roig A, et al. 2014. Biochar's role in mitigating soil nitrous oxide emissions: a review and meta-analysis. *Agriculture, Ecosystems & Environment* 191:5−16
[73] Surey R, Schimpf CM, Sauheitl L, Mueller CW, Rummel PS, et al. 2020. Potential denitrification stimulated by water-soluble organic carbon from plant residues during initial decomposition. *Soil Biology and Biochemistry* 147:107841
[74] Lan T, Li M, He X, Yuan J, Zhou M, et al. 2023. Effects of exogenous carbon and nitrification inhibitors on denitrification rate, product stoichiometry and *nirS*/*nirK*-type denitrifiers in a calcareous soil: evidence from ^{15}N anaerobic microcosm assays. *Journal of Soils and Sediments* 23:1217−1232
[75] Surey R, Lippold E, Heilek S, Sauheitl L, Henjes S, et al. 2020. Differences in labile soil organic matter explain potential denitrification and denitrifying communities in a long-term fertilization experiment. *Applied Soil Ecology* 153:103630
[76] Clough TJ, Condron LM, Kammann C, Müller C. 2013. A review of biochar and soil nitrogen dynamics. *Agronomy* 3:275−293